ISBN: 978-3-95450-191-5 doi:10.18429/JACoW-SRF2017-MOPB065

DEVELOPMENT OF HYBRID SUPERCONDUCTING PHOTOCATHODES ON NIOBIUM USING HIGH QE COATINGS

M. Warren†, Z. Yusof, L. Spentzouris, N. Samuelson, A. Denchfield, J. Zasadzinski,
Physics Department, Illinois Institute of Technology, Chicago, IL 60616, USA
W. Gai, E. Wisniewski, J. Shao, AWA, Argonne National Lab, Argonne, IL 60439, USA

Abstract

The quantum efficiencies (QE) and other relevant properties of photocathodes consisting of bulk Nb substrates coated with thin films of Cs_2Te and Mg are reported. Using the standard recipe for Cs_2Te deposition developed for Mo substrates (220 Å Te thickness), a QE ~11% - 13% at light wavelength of 248 nm is achieved for the Nb substrates, consistent with that found on Mo. Systematic reduction of the Te thickness for both Mo and Nb substrates reveals a surprisingly high residual QE ~ 6% for a Te layer as thin as 15 Å. A theoretical investigation based on the Spicer 3-Step model along with a solution of the Fresnel equations for reflectance, *R*, leads to a reasonable fit of the thickness dependence of QE and suggests that layers thinner than 15 Å may still have reasonably high QE. Such an ultra-thin, semiconducting Cs_2Te layer may be expected to produce sharp electron bunches with minimal ohmic losses for RF frequencies ~ 1 GHz.

For Nb/Mg bilayers dark current measurements up to 60 MV/m were obtained at the Argonne Wakefield Accelerator test station and fitted using Fowler-Nordheim theory. Enhanced field emission is likely due to surface roughness of the Nb substrate. The Mg layer appears to be robust down to 10 nm with no serious damage in high fields. A factor of 10 increase in QE over the bare Nb is found without any surface treatment of the Mg.

INTRODUCTION

Future free-electron-laser (FEL)-based light sources will require low emittance, high brightness and high average-current electron beams, necessitating high duty cycle (> 1 MHz) or effectively CW operation [1]. Superconducting radiofrequency (SRF) photoinjectors made of pure Nb are currently a favored choice for producing such beams as they dissipate significantly less power than normal RF guns [2]. The photocathode is an integral component of the photoinjector, contributing to the surface RF impedance, and therefore ideally it should be superconducting as well. A replaceable, superconducting plug cathode would be particularly attractive for a compact SRF linac as it has a simple design [2,3]. Recent advances in Nb-based SRF cavities, including record high Q values at 15-20 MV/m via a nitrogen doping process [4], as well as the successful in-situ growth of higher T_C Nb_3Sn on the inside surface [5, 6] suggests that a compact electron linac operating at 4.2 K is feasible in the future. The limiting factor is that the current choices of superconducting photocathode have relatively low quantum efficiencies (QE), e.g., for Nb QE < 0.01% and for Pb QE < 0.1% at 248 nm wavelength [3].

A potential way out of this difficulty is to consider hybrid structures whereby a thin film coating of a high QE material is deposited onto a bulk superconductor such as Nb or Nb_3Sn. For metallic overlayers, there is the phenomenon of the superconducting proximity effect which allows a thin, non-superconducting surface layer to acquire a Cooper pair condensate (zero dc resistance), and energy gap, via coupling to the underlying superconducting substrate [7,8]. Such an approach seems particularly attractive for thin films of Mg on Nb where earlier proximity effect studies have shown promising results [9]. Also, Mg has one of the highest QE values of any metallic element, ~ 0.1% at 248 nm. More detailed results on such Nb/Mg hybrid structures will be reported elsewhere [10].

High peak current is more easily obtained with semiconductor cathodes such as cesium telluride (Cs_2Te) [11,12]. It has a QE as high as 20% and has consistently produced a QE > 1% during normal accelerator operations over a period of at least a year, providing a relatively large bunch charge per laser pulse, and has been shown to be robust in a photoinjector environment. It has been used as an electron source in SRF photoinjectors, but only as a normal-state photocathode[13]. This requires a more complex engineering design to isolate the cathode from the rest of the superconducting cavity. It typically consists of an SRF cavity injector with a hole so that a high-QE normal photocathode can be introduced through a long rod, requiring an additional choke to minimize RF losses through the hole. Separate cooling and vacuum loading systems are also required. While this allows an electron pulse with high peak current, it is not clear if this method will meet the future needs of CW operation and, furthermore, may not be suitable for a compact linac.

Here we consider the use of Cs_2Te for a hybrid superconducting photocathode. Given that it is a semiconductor, the proximity effect might be weak or nonexistent. [7,8,9] However, even in the absence of any induced superconductivity, a very thin semiconducting surface layer may be highly transparent to the applied RF and contribute minimally to the surface impedance, which will still be determined predominantly by the underlying Nb substrate, while still providing the advantage of a higher QE than a metallic superconductor. Thus our study focuses on ultra-thin films of Cs_2Te on Nb substrates with thicknesses significantly less than the typical Te layer thickness (210Å) of Cs_2Te used in the standard "recipe" grown on a Mo substrate. The results thus far are reproducible and very encouraging. We find that the QE of Cs_2Te on Nb is nearly

† email: mwarren3@hawk.iit.edu

ISBN: 978-3-95450-191-5 doi:10.18429/JACoW-SRF2017-MOPB065

identical to that on Mo at the optimum Te thickness. While the QE drops with decreasing Te thickness, it still achieves a value of ~ 6% for the thinnest Te films (15 Å – 25 Å) studied to date. A theoretical analysis is presented which incorporates the Spicer 3-Step model of photoemission along with the Fresnel equations for the calculation of the optical reflectance R. Assuming QE is proportional to the transmittance (1-*R*), and substituting the electron diffusion length with film thickness, we find good agreement with experiment. The model suggests that even thinner layers might still give a reasonably high QE. Such ultra-thin Cs_2Te layers might be expected to produce sharp electron bunches. These results are quite promising for the development of a hybrid superconducting photocathode with high QE and low RF losses.

EXPERIMENT

Cs_2Te Film on Bulk Nb

Cs_2Te was fabricated at the Argonne Wakefield Accelerator (AWA) photocathode growth chamber. Details of the photocathode facility and the fabrication have been described in Ref. [14]. Briefly, the polished and cleaned substrate plug (typically Mo, but also Nb in this study) is mounted in an ultra-high vacuum chamber with base pressure of 2×10^{-10} Torr. The plug is kept at 120 C throughout the photocathode deposition. Te is deposited first, to the desired thickness, and monitored by a quartz-crystal thickness monitor. This is then followed by the deposition of Cs onto the Te layer whereby Cs_2Te is formed by a diffusion process. During the Cs deposition, the photocurrent generated by a filtered UV lamp (248 nm) is monitored by applying a positive bias to an anode near the photocathode surface. The deposition continues until the photocurrent reaches a peak value and saturates, upon which the Cs evaporation is halted. Previous depositions of Cs_2Te on Mo using the standard recipe with Te thickness of 210 A have produced peak as-deposited QE in the range of 8%-20% [14], with the majority falling between 10%-15%, at 248 nm wavelength.

Here the Mo plug has been substituted by Nb plug as the substrate. Cs_2Te deposited on Nb using the standard recipe (Te thickness = 210 A and labelled as Te210) has the similar QE to that deposited on Mo. Figure 1 shows the profile of the QE during Cs deposition for various Te thicknesses, including Te210 on Nb. The result shows that Cs_2Te on Nb is consistent with what was observed on a Mo substrate for the standard recipe. We next investigated Cs_2Te photocathodes on both Mo and Nb with a series of reduced Te thicknesses. The 25 A (Te25) and 15 A (Te15) on Nb are shown in Fig. 1. With cesiation the QE reaches a peak between 5% and 6%. These values are considerably higher than those found from a typical metal.

To confirm that the high QE is due to the thin layer of Cs_2Te, the Nb substrate is cesiated without any Te layer (Te0). The QE is considerably lower, never reaching above 1%, implying that a cesiated Nb surface cannot achieve such high QE. Thus, the elevated QEs that we measured for Te25 and Te15 were predominantly from the Cs_2Te layer on the Nb.

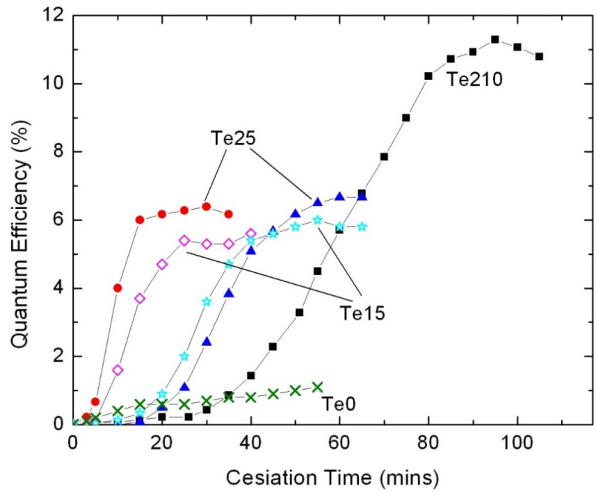

Figure 1: QE evolution of Cs_2Te photocathode on Nb substrate during Cs deposition. Te210 means the cesiation was performed after 210 A Te film was deposited, while Te25 and Te15 were done on 25 A and 15 A, respectively. Te0 is a cesiated Nb surface with no Te deposition.

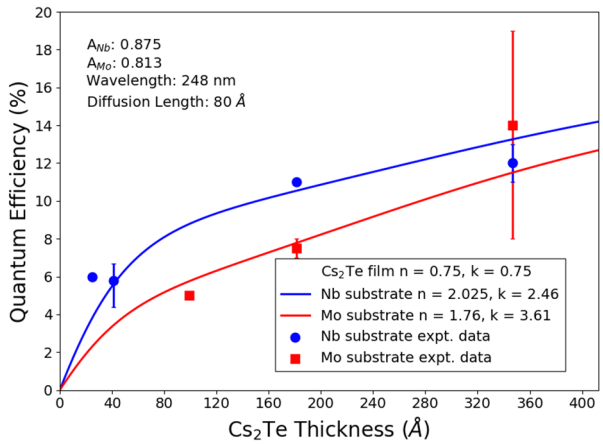

Figure 2: Dependence of the quantum efficiency (QE) of Cs_2Te films on Nb (blue circles) and Mo (red squares) substrates vs. Cs_2Te thickness. Data points correspond to the average values while error bars represent the maximum and minimum measured QE for any given thickness. Solid curves are the theoretical model fits described in the text using *n* and *k*, the real and imaginary parts of the index of refraction, respectively.

The combined results of QE vs. Te thickness for Nb and Mo substrates are shown in Fig. 2. As reported by other groups, Cs2Te has shown a wide variation in QE under the same deposition technique. This has been observed here as well, especially for Cs2Te with the standard thickness of Te=210A. Both substrates show a decrease of QE for Te thicknesses below the optimal value of 210 Å but the combined data indicate that the slope is weak. In addition, the QE for ultra-thin Cs_2Te between 5%-7% is reproducible.

ISBN: 978-3-95450-191-5 doi:10.18429/JACoW-SRF2017-MOPB065

Analysis of the data shown in Fig. 2 is achieved by using the Spicer 3-Step model for photoemission.[15] Briefly, this model breaks down the overall process into three separate parts: *i.* absorption of photon (characterized by absorption coefficient, α) and generation of excited electron, *ii.* diffusion of excited electron to the vacuum interface characterized by diffusion length, *L* and *iii.* escape of electron from surface, typically via tunneling which is strong when the electron energy E-E_F is ~ work function, *W*. For E-$E_f > W$ the process involves a scattering of the electron at the vacuum interface. These individual processes each involve probabilities which we have subsumed into an overall scale factor in the following expression.

$$QE = A(1-R)\left(\frac{1}{1+\frac{1}{\alpha L}}\right). \quad (1)$$

The scale factor *A* is a property solely of the Cs_2Te film. [15] This factor is treated as a lone free parameter but we note its value is consistent for Mo and Nb substrates. All other terms are determined from the optical constants of Nb (or Mo) and Cs_2Te and the measured Te film thickness. Note Fig. 1 labels data with the measured Te thickness whereas Fig. 2 accounts for the larger unit cell volume of the Cs_2Te.

Since the Spicer model is developed for a single, relatively thick homogeneous material, it is worthwhile to discuss how the model is affected in the bilayer system studied here. First, the transmission coefficient at the Cs_2Te surface (1-*R*), essentially the fraction of incident photons entering the photocathode, is affected by both the film and the underlying substrate and thus the Fresnel equations are used to determine this value assuming a single optical reflection off the substrate (Nb or Mo). This reflection, R_{sub}, is found using the complex index of refraction (real part *n*, imaginary part *k*) of the substrate as indicated in legend of Fig. 2. The Fresnel equations are solved using an open source program created by Dr. Steven Byrnes [16], called Transfer Matrix Method (TMM) [17]. Used as input for the program are the measured Te thicknesses of the thin film layers and their complex indices of refraction of Cs_2Te [18]. In this system, we have a thin film layer of Cs_2Te on top of a much thicker layer of either Nb or Mo as a 3 mm substrate. The aforementioned parameters are used in the TMM to derive the reflectance *R* from a layer, which can then be used in eq. 1 to derive the QE of the multilayer system.

An important approximation used in Eq. 1 involves the diffusion length, *L*, of the photogenerated carriers, which is the average distance traveled by carriers heading to the surface before recombination. For Cs_2Te film thickness much less than *L*, we replace *L* with film thickness, since only carriers generated within the film contribute to QE. For d>L we use the value of L = 8.0 nm [19]. This can be justified further by noting that the substrates generally have much lower QE (by at least two orders of magnitude) and are effectively not participating in any processes relevant to the measured, much higher, QE values.

The fit curves in Fig. 2 are reasonably good and explain well several features of the data. First, for a given thickness of Cs_2Te the QE for Nb substrates is generally higher than for Mo and appears to originate in the reflection off the substrate. More importantly, Eq. 1 shows that in the limit of $\alpha L << 1$, the QE is proportional to $L=d$, the thickness of the film. This crossover to the linear region occurs for film thickness < 5 nm, and this explains the relatively weaker slope found for thicknesses from 5-25 nm. Furthermore, the model indicates that reasonable QE values ~ 2% could be found with Te thicknesses as small as 5 Å.

Mg Film on Bulk Nb

Cathode plugs were designed and fabricated, for testing at the AWA test stand. Mg films were prepared at the Illinois Institute of Technology via a physical vapor deposition process similar to that of Cs_2Te described above. The substrate consisted of a pure Nb disk ~0.8 in. in diameter. The Nb substrate was polished using a diamond slurry polishing solution. Before deposition, the disks were mounted to a Mo heater block. Under ultra-high vacuum pressure conditions (10^{-8} torr), the substrate was annealed at 600 C for 8 hours to remove the oxide layer and then allowed to cool. The Mg film was deposited with the substrate at room temperature. Thickness was monitored with a quartz crystal thickness monitor. Two thicknesses were produced in order to test the viability of an ultra-thin Mg film (1-10 nm) cathode as compared to bulk Mg thicknesses (100nm-1μm).

The QE and work function was measured for each sample in a dedicated chamber under 10^{-4} torr pressures. QE was measured by illuminating the cathode with a UV lamp and filter with a peak wavelength λ : 248 nm. An anode is place 20 mm away from the sample and kept at a 450V bias to measure photocurrent with a Keithley picoameter. Work functions measurements were made with a Kelvin probe mounted in the same chamber. These values are listed in Table 1.

Table 1: Measured Values of Nb/Mg

Mg Film Thickness (nm)	QE	Work Function (eV)
0	1 x 10^{-6}	4.1
10	1.5 x 10^{-5}	3.81
100	9.0 x10^{-5}	3.7

ISBN: 978-3-95450-191-5 doi:10.18429/JACoW-SRF2017-MOPB065

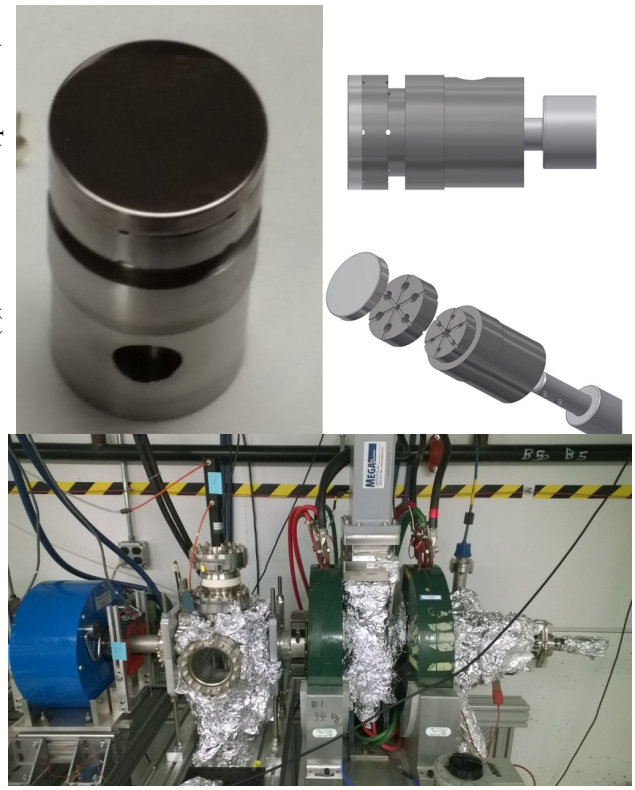

Figure 3:Top Left: Fabricated Mg thin film cathode on Nb disk mounted to stainless steel plug. Top Right: Modular assembly design of cathode plug with Nb disk face. Bottom: AWA test stand at Argonne National Labs.

Each cathode disk was designed to be mounted to a stainless steel plug to be inserted in the AWA test stand. The initial test was to determine the viability of such a thin Mg film under RF conditions (50 MV/m). The test stand itself is a single cell 1.3 GHz Cu pillbox RF cavity with a bucking and focusing solenoid. Downstream from the cavity is a rectangular Al Faraday cup. This gives the capability to measure the field emission current of the cathode. Therefore each thickness of Mg measured along with a "blank" Nb cathode as well as a solid Cu cathode plug of the same design parameters. The Mg cathodes were successfully conditioned to gradients as high as 60 MV/m without damaging the cathode surface. Although breakdown did occur during conditioning, it occurred primarily at the edge of the cathode plug where the applied RF field is geometrically enhanced due to sharp edges. For each cathode test, Field Emission data was recorded once a dark current value could be detected with the experimental apparatus.

The field emission data was analysed via Fowler Nordheim theory under RF fields [20] which describes the relation between field emission currents and applied field by

$$\frac{d(\frac{log_{10}I_F}{E^{2.5}})}{d(\frac{1}{E})} = -\frac{2.84x10^9\phi^{1.5}}{\beta}. \quad (2)$$

Where I_F is the field emission current, E the applied field, ϕ the work function. The assumptions made were a uniform field over half of rf period (likely an overestimation), charge was emitted uniformly over the entire rF pulse. β values were extracted from the linear fit of Figure 5 derived from the left side of Equation 2 and we suspect the large values are due to surface roughness of the polished Nb substrate.

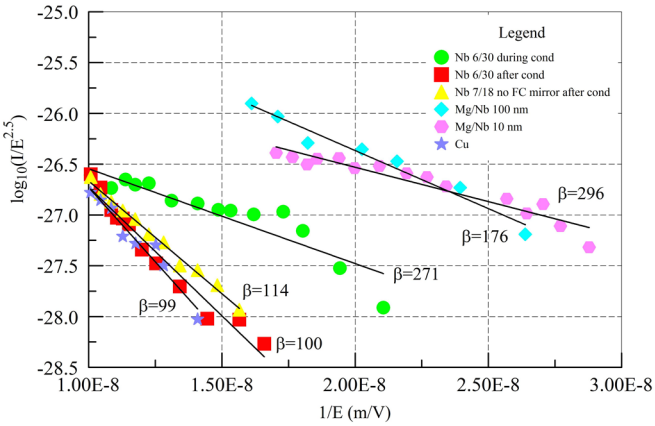

Figure 4: Fowler Nordheim fitting of each cathode. The Nb cathode was fit both during cathode conition (RED) and after conditioning (GREEN).

CONCLUSION

This research represents the initial stages of an investigation into the use of hybrid structures consisting of high QE metal and semiconductor coatings on Nb for the development of superconducting photocathodes. Results so far are very encouraging. For the Cs2Te coatings a surprisingly large value of QE ~ 5-6% is found for thicknesses < 4 nm, consistent with a phenomenological fit based on the Spicer model. This suggests that even thinner layers (5 Å Te thicknees) would still provide QE ~ 1% or higher. The ultra thin Cs2Te might be expected to produce minimal RF losses. For the Mg coatings, which would be robust in air, we find that the thinnest layer, 1.0 nm, displays a work function near that of bulk Mg, and a ten-fold increase in QE over bare Nb, even without any surface treatment. The Mg layer is also robust up to 60 MV/m RF fields. Dark current measurements show a field enhancement which is attributed to residual surface roughness of the polished Nb surface.

ACKNOWLEDGMENT

We acknowledge the use of AWA photocathode growth facility, including valuable support and assistance from Manoel Conde and Eric Wisniewski. ZY and MW acknowledge assistance from and discussion with Daniel Velazques. The AWA is funded US Dept. of Energy Office of Science under Contract No. DE-AC02-06CH11357. ZY is supported by US Dept. of Energy under Grant No. DE-SC0007952. MW is supported by Department of Energy SCGSR Award under contract DE - AC05 - 06OR23100. This work was funded in part by the Department of Energy under the grant no. DE-SC0015479.

ISBN: 978-3-95450-191-5 doi:10.18429/JACoW-SRF2017-MOPB065

REFERENCES

[1] Science and Technology of Future Light Sources, a White Paper (2008) https://inspirehep.net/record/817775/files/slac-r-917.pdf.

[2] A. Arnold and J. Teichert, *PRST-AB* 14,024801 (2011).

[3] J. Smedley, T. Rao, J. Sekutowicz, *PRST-AB* 11, 013502 (2008).

[4] A. Grassellino, A. Romanenko, D. A. Sergatskov, O. Melnychuk, Y. Trenikhina, A. C. Crawford, A. Rowe, M. Wong, T. Khabiboulline, F. Barkov, *Supercond. Sci. Tech*., 26, 102001 (2013).

[5] S. Posen and D.L. Hall, Supercond. *Sci. Technol*. 30, 033004 (2017).

[6] Chaoyue Becker, Sam Posen, *et al*, *Appl.Phys.Lett.* 106, 082602 (2015).

[7] E.L. Wolf, J. Zasadzinski, J.W. Osmun and G.B. Arnold, "Proximity Electron Tunneling Spectroscopy I. Experiments on Nb", *Journal of Low Temp. Physics,* 40, 19 (1979).

[8] J. Zasadzinski, D.M. Burnell, E.L. Wolf and G.B. Arnold, "Superconducting Tunneling Study of Vanadium", *Phys. Rev.* B 25, 1622 (1982).

[9] D.M. Burnell, E.L. Wolf, J. *Low Temp. Phys*., 58, 61 (1984).

[10] M. Warren, *et al*., (in preparation).

[11] S.H. Kong, *et al.*, *Nucl. Inst. Meth*. A 358, 276 (1995).

[12] P. Michelato, *et al., Nucl. Inst. Meth.* A 393, 464 (1997).

[13] R.Xiang, A.Arnold, H.Buettig, D.Janssen, M.Justus, U.Lehnert, P.Michel, P.Murcek, A.Schamlott, Ch.Schneider, R.Schurig, F.Staufenbiel, J.Teichert, *Phys. Rev. STAB*, 13, 043501 (2010).

[14] Z. Yusof et al., Proc. IPAC12, 1569 (2012).

[15] Berglund and Spicer, *Phys. Rev. A* 136, 1030 (1964).

[16] S.J. Byrnes, arXiv:1603.02720 [physics.comp-ph].

[17] Charalambos C. Katsidis and Dimitrios I. Siapkas, *Appl. Opt.* 41, 3978-3987 (2002).

[18] P. Michelato, L. Monaco, D. Sertore, S. Bettoni, "Optical Properties of Cesium Telluride", in *Proc. EPAC'02*, Paris, France, June 2002, paper 1810.

[19] G. Ferrini, P. Michelato and F. Parmigiani, Solid State Communications, Vol. 106, No. 1, 21 (1998).

[20] J.W. Wang and G.A. Loews SLAC-pub-7684 (1997).